SIMULTANEOUS DETERMINATION OF ACOUSTIC IMPEDANCE, LONGITUDINAL AND LATERAL WAVE VELOCITIES FOR THE CHARACTERIZATION OF THE ELASTIC MICROSTRUCTURE OF CORTICAL BONE

K. Raum and J. Brandt
Q-BAM Group, Dept. of Orthopedics, Martin Luther University of Halle-Wittenberg, Halle, Germany
kay.raum@medizin.uni-halle.de

Abstract

A highly focussed 50 MHz broadband transducer was used to generate longitudinal and lateral waves in thin cortical bone sections. The pulse-echo trays of the reflections from the front and back sides of the sample were recorded as a function of the transducer-sample distance *V(z,t)*. After pulse separation the confocal positions of the individual echoes and their corresponding times-of-flight were determined. From these values the sample thickness as well as longitudinal and lateral sound velocities were determined using a specially developed iterative analysis algorithm. The confocal surface echo amplitude was used to obtain the acoustic impedance. With these quantities the mass density and elastic parameters were derived. The relations between acoustic elastic properties were examined.

Introduction

High frequency ultrasound has been used for the characterization of the elastic microstructure of bone for more than two decades now. The acoustic impedance Z as well as the longitudinal sound velocity v_l appeared to be sensitive to variations of bone elasticity. While two-dimensional impedance maps are usually derived from confocal surface reflectivity scans, v_l has been measured in thin samples both in transmission and reflection, and in thick samples with the so-called *V(z)* technique, respectively. However, crucial parameters for the velocity estimation (sample thickness) and for the derivation of elastic parameters (density, Poisson ratio) were mostly adopted from macroscopic measurements or literature values. On the other hand the possibility of the simultaneous determination of sample thickness and sound velocity with highly focussed ultrasound has been demonstrated in polymers and biological soft tissues, both for transmission and pulse-echo operation [1,2].

A spherically focussed sound field can generate Rayleigh, longitudinal and shear waves at a fluid-solid boundary (Fig. 1). Refraction of the transmitted waves is determined by Snell's law. In thin samples these waves can be reflected at the rear side of the solid and propagate back to the transducer. If the focal plane of the sound field coincides with the sample front surface, all of the incident waves are in phase and the reflected amplitude reaches a maximum. The confocal time of flight (*TOF*) is:

$$TOF_1 = \frac{2F}{v_0}, \tag{1}$$

whereas v_0 is the speed of sound in the coupling fluid and F is the focal distance. The amplitude is proportional to the reflection coefficient, from which the acoustic impedance can be derived [3]. When the transducer is moved towards the sample, both the shear wave and the longitudinal waves will successively focus on the rear surface. The TOF of the confocal rear reflection of the longitudinal wave is:

$$TOF_2 = \frac{2F}{v_0} - \frac{2\overline{AC_l}}{v_0 \cos\alpha} + \frac{2\overline{AC_l}\cdot v_0}{v_1^2 \cos\alpha}. \tag{2}$$

α is the semi-aperture angle of the incident sound field and $\overline{AC_l}$ the necessary transducer displacement to focus from front to the rear side of the sample. Sound velocity and sample thickness are then determined by Eq. (3) and (4):

$$v_1 = \left[\frac{v_0^2}{1 - \frac{(TOF_1 - TOF_2)\cdot v_0 \cdot \cos\alpha}{2\overline{AC_l}}} \right]^{1/2}, \tag{3}$$

$$d = \frac{\overline{AC_l}}{\frac{1}{2}\frac{v_1}{v_0}\left(1 - \frac{v_1^2}{v_0^2}\right)\cdot(1-\cos\alpha) - \frac{v_1}{v_0}}. \tag{4}$$

When the shear wave is focussed on the rear side, lateral stress components are extinguished and the remaining normal stress components generate a longitudinal wave. The TOF of this reflected pulse is:

$$TOF_3 = \frac{2F}{v_0} - \frac{2\overline{AC_s}}{v_0 \cos\alpha} + \frac{\overline{AB}}{v_1 \cos\beta_s} + \frac{\overline{AB}}{v_s \cos\beta_s}, \tag{5}$$

whereas $\overline{AC_l}$ is the transducer displacement to focus from the front surface to the rear shear wave focus, $\overline{AB}$ is equal to the sample thickness d, and β_s is the angle of refraction. The shear wave velocity is obtained from:

$$v_s = \frac{d}{\left(\frac{2\overline{AC_s}}{v_0\cdot\cos\alpha} - \frac{d}{v_l\cdot\cos\beta_s} - (TOF_1 - TOF_3)\right)\cdot\cos\beta_s}. \tag{6}$$

If the difference of the sound velocities in the coupling fluid and the solid is large, spherical aberration

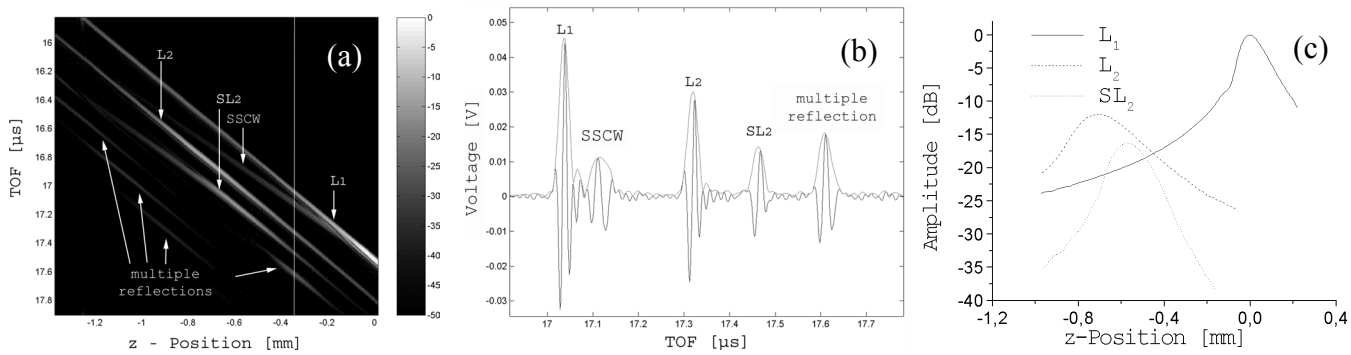

Figure 1 : In the *V(z,t)* image (a) the envelope of the pulse-echo tray of successive front and rear surface reflections (b) are plotted as a function of the transducer-sample distance. Brightness corresponds to signal amplitude in dB. The diagonal lines indicate the individual echoes: L_1 - longitudinal wave front side reflection, SSCW - surface skimming compressional wave, L_2 - longitudinal wave rear side reflection, SL_2 - shear wave rear side reflection (shear wave transmission, longitudinal wave reflection). The defocus position of the pulse-echo in (b) is marked as a vertical line in (a). After pulse separation the V(z) curves and corresponding TOF's can be reconstructed (c). The measurement was made in a PMMA sample (thickness: 390 µm).

as well as the angular dependent energy flux have to be considered. While spherical aberration tends to shift the true focus towards the paraxial focus, the angular dependent energy flux causes an apodization of the incident field. These effects are taken into account by an iterative analysis algorithm. A comprehensive description can be found elsewhere [4].

Methods

Samples

Homogenous polymers served as reference materials (Teflon®, polystyrene, polycarbonate, polymethylmethacrylate (PMMA)). The longitudinal sound velocity v_l was determined with a broadband V(z)-technique [5] and mass density by Archimedes' principle, respectively (see Table 1).

Table 1 : Density and longitudinal sound speed of the reference materials were determined with alternate techniques (*for Teflon® manufacturer specifications were used). The values in the brackets were determined with the proposed technique.

	v_l [m/s]	ρ [kg/m³]
Teflon®	1390*	2150*
	(1376 ± 16)	(2141 ± 15)
polystyrene	2266 ± 4	1048
	(2248 ± 11)	(1068 ± 9)
polycarbonate	2306 ± 10	1197
	(2298 ± 6)	(1222 ± 21)
PMMA	2640 ± 4	1184
	(2641 ± 6)	(1199 ± 4)

Proximal cortical bone sections were obtained from human cadaver femora approximately 10 cm beneath the femoral head. After dehydration the specimen were embedded in PMMA. The samples were cut parallel or perpendicular to the femoral long axis and thin sections with smooth surfaces were prepared by grinding and polishing the surfaces from both sides down to a thickness between 100 and 300 µm.

Experimental Setup

A custom scanning acoustic microscope (Q-BAM, Halle, Germany) was used. It consists of a 3 axis high precision scanning stage, a 200 MHz pulser/receiver (Panametrics 5900PR) and a 500 MS/s A/D-card (Gage 8500). All components are controlled by a custom software. A spherically focused transducer (V605: Valpey Fisher, Hopkinton, USA) with an aperture of 60° was used. The pulse-echo sound field parameters were determined with the wire technique [6] and are summarized in Table 2.

Table 2 : Sound field parameters of the V605 transducer.

center frequency f_c	49.0 MHz
fractional bandwidth	84.3 %
f-number $f^{\#}$	1
Focus distance F	6350 µm
beam width D_{lat}	23 µm
depth of focus F_z	169 µm

The samples were attached to special sample holders with 4 mm holes in order to have a well defined sample/water interface at the rear surface. For the measurement sample and holder were completely immersed in a temperature controlled tank filled with distilled, degassed water at 25°C. The front surfaces were scanned in C-scan mode for the selection of measurement locations. Spots with a large distance to structural boundaries were chosen for the evaluation.

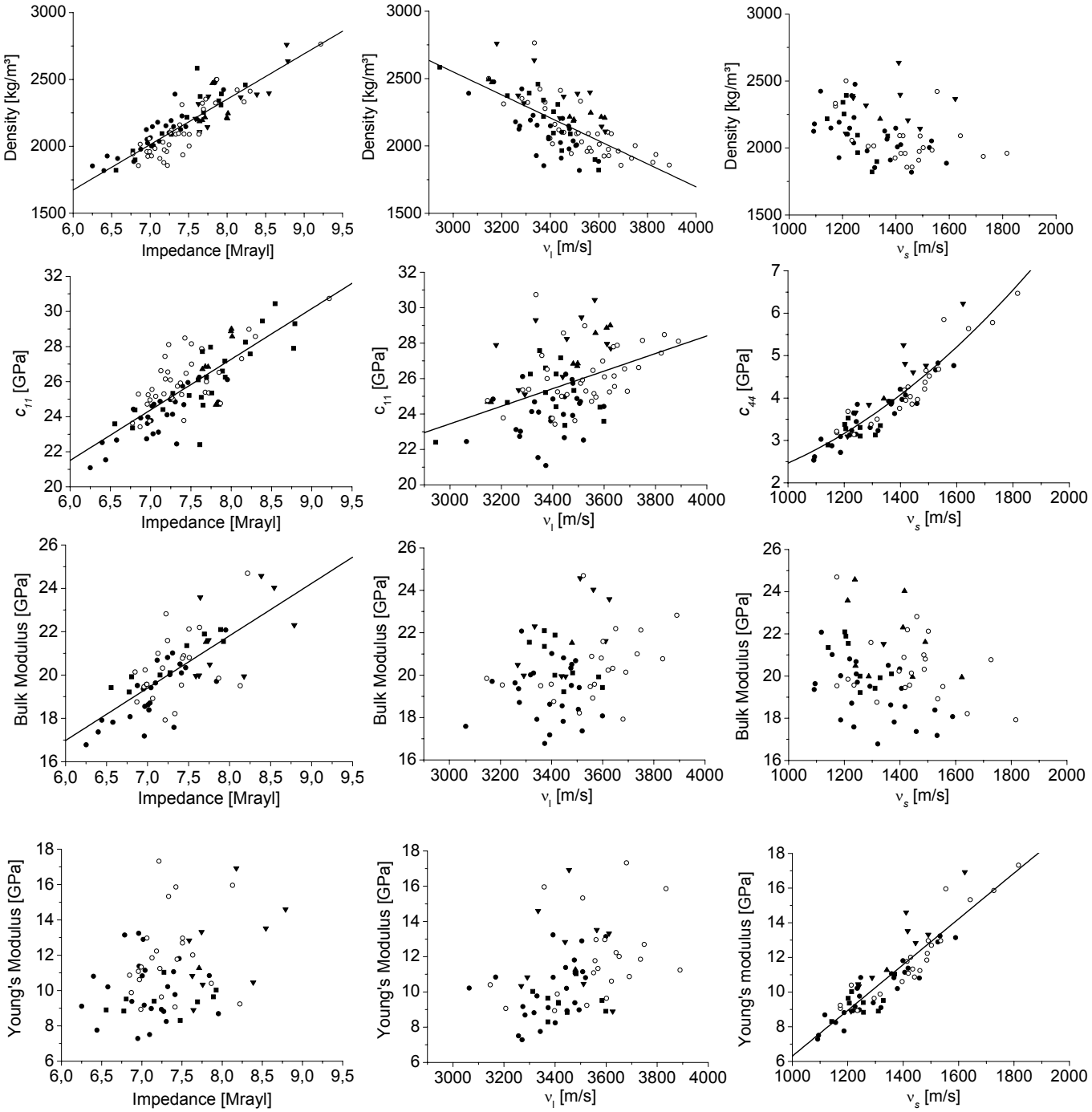

Figure 2 : Correlations between acoustic and elastic properties (hollow dots: samples with 90° orientation; filled dots: samples with 0° orientation). Significant correlations are indicated with solid lines.

V(z,t) Measurement

The pulse-echo trays of the front and rear surface reflections were recorded as a function of the transducer-sample distance with a *z*-increment of 4 µm (Fig. 1). For each scanned point the entire pulse echo signal was stored.

After pulse separation using a Hanning window (width: 2 x pulse duration) the individual echoes were Fourier-transformed. The V(z) curves were reconstructed for the center frequency (Fig. 1(c)) and the TOF's were determined using a phase sensitive technique [4,7]. This procedure ensured the exclusion of artefacts due to frequency dependent attenuation in the sample. The confocal locations of the L_1, L_2, and SL_2 pulses and their corresponding TOF's were determined at the zero crossing of the first derivative of *V(z)*.

The acoustic impedance was determined from the calibrated confocal front surface reflection amplitude and the sound velocities using equations (3) to (6). A specially developed iterative analysis algorithm accounts for a reduction of the effective aperture due to an angular dependent energy transmission.

Parameter Estimation

Mass density and isotropic elastic parameters were derived using the following equations:

Density: $\rho = \frac{Z}{v_l}$

Stiffness: $c_{11} = Z \cdot v_l$

Shear modulus: $c_{44} = \rho \cdot v_s^2$

Bulk modulus: $B = c_{11} - \frac{4}{3} c_{44}$

Young's modulus: $E = c_{44} \cdot \frac{3c_{11} - 4c_{44}}{c_{11} - c_{44}}$

Poisson ratio: $\sigma = \frac{1 - 2\,c_{44}/c_{11}}{2\left(1 - 2\,c_{44}/c_{11}\right)}$

Results

The means, standard deviations and ranges of the measured and derived parameters are summarized in Table 3. Figure 2 shows the relations between acoustic and elastic quantities. The acoustic impedance correlated with density ($R^2 = 0.752$), stiffness ($R^2 = 0.616$), and Bulk modulus ($R^2 = 0.520$). Only density and stiffness were correlated with the longitudinal sound speed. However, the correlation coefficients were lower compared to the correlations with Z ($R^2 = 0.465$ and $R^2 = 0.177$). Good correlations were found between shear velocity and shear modulus ($R^2 = 0.847$) and Young' modulus ($R^2 = 0.832$). The correlations of Young's modulus with impedance, longitudinal sound velocity and density were not significant.

Stepwise multiple regression statistics was applied to the data in order to quantify the prediction power of parameter combinations. The prediction of the Bulk modulus was improved in 2-parameter combinations of ρ orv_l with Z from $R^2 = 0.594$ (Z only) to $R^2 \approx 0.67$.

Moderate but significant predictions of Young's modulus was achieved with the combinations Z-v_l ($R^2 = 0.310$), v_l-ρ ($R^2 = 0.314$), and Z-ρ ($R^2 = 0.300$).

Table 3: Means, standard deviations and ranges of acoustic and elastic parameters.

	mean	std	min	max
Z [Mrayl]	7.44	0.54	6.25	9.22
v_l [m/s]	3451	168	2944	3890
v_s [m/s]	1352	155	1092	1816
ρ [kg/m³]	2164	210	1818	2764
c_{11} [GPa]	25.68	1.97	21.09	30.74
c_{44} [GPa]	3.90	0.86	2.53	6.47
E [GPa]	10.96	2.24	7.28	17.32
B [GPa]	20.19	1.71	16.78	24.69
σ	0.41	0.02	0.34	0.44

Conclusions

With the proposed method the derivation of isotropic elastic parameters is possible. Due to the one-dimensional measurement and limited spatial resolution this technique is not suitable for extensive studies of the heterogeneous microstructure. However, it provides valuable information about principal relations between acoustic and elastic quantities.

Statistic analysis showed that none of the commonly used parameters for the prediction of bone elasticity (ρ,v_l) correlated with the elastic modulus E. Moreover no parameter appeared to be constant within the heterogeneous bone matrix. Therefore a full elastic characterization of the microstructure requires the measurement or derivation of all necessary parameters. The acoustic impedance seemed to be suitable for the prediction of elastic stiffness and Bulk modulus. By combining two parameters statistically significant models with moderate prediction power for the Young's Modulus were found. The most promising combination could be impedance-density, since both quantities can be measured easily in two dimensions with a high spatial resolution.

References

[1] Haenel,V., "Measurement of sound velocity and thickness of thin samples by time-resolved acoustic microscopy," *J. Appl. Phys.*, vol. 84, pp. 668-670, 1998.

[2] Maev,R.G. and Levin,V.M., "Principles of local sound velocity and attenuation measurements using transmission acoustic microscope," *IEEE Trans. Ultrason. , Ferroelect. , Freq. Contr.*, vol. 44, pp. 1224-1231, 1997.

[3] Hirsekorn,S., Pangraz,S., Weides,G., and Arnold,W., "Erratum: Measurement of elastic impedance with high spatial resolution using acoustic microscopy," *Appl. Phys. Lett.*, vol. 69, pp. 2138, 1996.

[4] Raum,K., "Quantitative Akustische Rastermikroskopiemethoden zur Charakterisierung der elastischen Eigenschaften von Knochengewebe." Thesis, Halle, 2002.

[5] Raum,K. and Brandt,J., "High-frequency acoustic dispersion of surface waves using time-resolved broadband microscopy," in *Proc. IEEE Ultrason. Symp.*, 2003, in press.

[6] Raum,K. and O'Brien,W.D., "Pulse-echo field distribution measurement technique for high-frequency ultrasound sources," *IEEE Trans. Ultrason. , Ferroelect. , Freq. Contr.*, vol. 44, pp. 810-815, 1997.

[7] Kim,T.J. and Grill,W., "Determination of the velocity of ultrasound by short pulse switched sinusoidal excitation and phase-sensitive detection by a computer-controlled pulse-echo system," *Ultrasonics*, vol. 36, pp. 233-238, 1998.